The Geology and Tectonics of central Bhutan

Supplementary File B: Sample Catalogue and Descriptions

Lucy Greenwood[1], Tom Argles[1*], Randy Parrish[2,3], Nigel Harris[1], Clare Warren[1]

[1] Department of Environment, Earth and Ecosystems, Centre for Earth, Planetary, Space and Astronomical Research (CEPSAR), The Open University, Walton Hall, Milton Keynes, MK7 6AA, United Kingdom

[2] Department of Geology, University of Leicester, University Road, Leicester, LE1 7RH, United Kingdom

[3] NERC Isotope Geosciences Laboratory, British Geological Survey, Keyworth, Nottingham NG12 5GG, United Kingdom

* corresponding author (e-mail: tom.argles@open.ac.uk)

This appendix includes a tabulated sample catalogue with information on sample locations, lithology and mineralogy, petrographic descriptions of metapelitic samples at localities either referred to in the narrative or else for general reference and background information, including representative garnet profiles in samples from various units.

1. Sample catalogue

Common abbreviations

Geological units and structure

TSS	Tethyan Sedimentary Series
GHS	Greater Himalayan Series
LHS	Lesser Himalayan Series
STD	South Tibetan Detachment

Mineral abbreviations

gt	garnet
sill	sillimanite
ky	kyanite
st	staurolite
bi	biotite
mu	muscovite

MCT	Main Central Thrust	tur	tourmaline
		qtz	quartz
		ox	oxides
		fsp	feldspar
		chl	chlorite
		ap	apatite
		amp	amphibole
		cc	calcite
		rut	rutile
		trem	tremolite

Notes on Table C.1 (below): longitude and latitude are in decimal degrees; shaded boxes indicate mineral present.

Table C.1 Sample catalogue

	GPS			Field Analysis		Mineralogy															
Locality No.	Latitude	Longitude	Elevation/*m*	Unit	Lithology	gt	sill	ky	st	bi	mu	tur	qtz	ox	fsp	chl	ap	amp	cc	rut	trem
LG-09- 1	27.48612	89.91515	1365	GHS	gneiss	■	■	■		■	■		■	■	■						
LG-09- 2	27.49622	90.03883	1692	GHS	orthogneiss	■				■	■		■	■	■	■	■				
LG-09- 3	27.49858	90.05839	1791	TSS	schist					■	■	■	■								
LG-09- 4	27.50350	90.08108	1946	TSS	phyllite	■				■	■	■	■								
LG-09- 6	27.47178	90.47928	2263	GHS	schist	■	■	■	■	■	■	■	■	■	■		■				
LG-09- 7a	27.47178	90.47928	2263	TSS	pegmatite				■	■			■		■						
LG-09- 7b	27.47178	90.47928	2263	TSS	orthogneiss					■			■		■						
LG-09- 7c	27.47178	90.47928	2263	TSS	pegmatite																
LG-09- 8a	27.48089	90.48325	2230	GHS	schist	■				■			■								
LG-09- 8b	27.48089	90.48325	2230	GHS	schist	■				■		■									
LG-09- 9a	27.41461	90.50883	1820	TSS	quartzite	■				■	■		■	■							
LG-09- 9b	27.41461	90.50883	1820	TSS	pelitic rich layer	■				■	■		■		■						
LG-09- 9c	27.41461	90.50883	1820	TSS	pelitic rich layer	■				■	■		■								
LG-09- 11	27.41260	90.51176	1774	TSS	schist								■	■	■			■			
LG-09- 12	27.42282	90.49230	1853	GHS	orthogneiss	■				■			■		■						
LG-09- 16	27.36851	90.53451	1133	TSS	quartzite					■			■								
LG-09- 21	27.28155	90.62450	1436	TSS	quartzite					■	■		■	■							
LG-09- 26	27.14777	90.68972	521	TSS	quartzite conglomerate					■			■		■						
LG-09- 27	27.14807	90.69118	541	TSS	quartzite																
LG-09- 32	27.11922	90.67465	818	TSS	schist	■				■	■		■	■							
LG-09- 40	27.04044	90.63630	1859	TSS	schist																
LG-09- 41	27.04065	90.63547	1748	TSS	schist																
LG-09- 42	27.03465	90.62971	1663	GHS	orthogneiss						■		■		■						
LG-09- 43a	27.03622	90.63198	1646	GHS	orthogneiss						■		■		■						
LG-09- 43b	27.03622	90.63198	1646	GHS	schist					■	■		■		■						
LG-09- 43c	27.03680	90.63226	1646	TSS	quartzite																
LG-09- 43d	27.03680	90.63226	1646	TSS	quartzite					■	■		■	■							
LG-09- 45	27.01706	90.61524	1654	GHS	granitoid intrusion					■			■		■						
LG-09- 46	27.01449	90.61523	1629	GHS	schist	■				■	■		■	■							
LG-09- 48b	26.99613	90.59676	1244	GHS	orthogneiss					■			■		■						
LG-09- 49a	27.00185	90.59254	1174	GHS	schist	■				■	■		■		■						
LG-09- 49b	27.00185	90.59254	1174	GHS	schist					■	■		■		■						
LG-09- 50a	27.01045	90.58817	1087	GHS	schist	■				■	■	■	■								
LG-09- 50b	27.01045	90.58817	1087	GHS	schist	■				■	■	■	■	■	■						
LG-09- 52	27.01034	90.58119	946	GHS	schist	■				■	■		■								
LG-09- 53	27.00231	90.55266	1193	GHS	schist	■				■			■		■						
LG-09- 53	27.00231	90.55266	1193	GHS	schist	■				■			■	■		■					
LG-09- 55	26.97261	90.54632	1216	GHS	schist	■				■	■	■	■		■						
LG-09- 57	26.95999	90.56097	1024	GHS	ultrmylonite																
LG-09- 59	26.90759	90.20956	872	LHS	quartzite																
LG-09- 59a	26.90759	90.20956	872	LHS	phyllite																
LG-09- 59b	26.90759	90.20956	872	LHS	quartzite																
LG-09- 60	26.91868	90.20420	1046	Jaishidanda	schist	■		■			■		■								
LG-09- 61a	26.92609	90.20744	1124	Jaishidanda	schist	■				■	■	■	■	■	■						
LG-09- 61b	26.92609	90.20744	1124	Jaishidanda	schist																
LG-09- 61c	26.92609	90.20744	1124	GHS	augengneiss	■				■	■		■		■						
LG-09- 65	26.96632	90.18357	1743	GHS	schist	■				■	■	■	■	■	■						
LG-09- 70a	27.03051	90.07346	332	GHS	paragneiss	■		■	■	■			■		■						
LG-09- 70b	27.03051	90.07346	332	GHS	paragneiss			■		■	■	■	■		■						
LG-09- 72a	27.09809	90.07538	546	TSS	quartzite					■	■	■	■								
LG-09- 72b	27.09809	90.07538	546	TSS	garnetiferous quartzite	■				■			■		■	■	■				
LG-09- 78	27.26200	90.03706	678	Leucogranite	bi-mu leucogranite					■	■		■								
LG-09- 82	27.44636	89.90680	1201	GHS	sill paragneiss		■			■	■		■	■	■						

Table C.1 Sample catalogue *cont.*

	GPS			Field Analysis		Mineralogy														
Locality No.	Latitude	Longitude	Elevation/*m*	Unit	Lithology	gt	sill	ky	st	bi	mu	tur	qtz	ox	fsp	chl	ap	amp	cc	rut	trem
LG-09- 85	27.45616	89.90549	1201	GHS	sill paragneiss		■			■	■	■	■		■						
LG-09- 86	27.46652	89.89794	1227	Paro	schist	■	■		■	■	■	■	■		■						
LG-09- 90	89.69466	27.42046	2554	GHS	paragneiss	■	■			■	■		■		■						
LG-09- 98	89.69724	27.37829	3836	GHS	paragneiss	■	■			■	■		■		■						
LG-09- 101	89.70560	27.37025	4250	GHS	schist	■	■			■	■		■		■						
LG-09- 104	89.72776	27.34897	4097	GHS	leucogranite	■				■	■		■		■						
LG-09- 110	89.70142	27.34572	3539	GHS	paragneiss	■	■			■	■		■		■						
LG-09- 118	89.66720	27.32722	3128	GHS	sill vein																
LG-09- 123	89.64322	27.32095	2882	Paro	qtz-metasediment																
LG-09- 142	89.35812	27.49273	3103	GHS	sill schist	■	■			■			■								
LG-09- 143	89.35936	27.48500	2748	GHS	sill schist	■	■			■			■		■						
LG-09- 144	89.36073	27.48558	2712	GHS	sill schist	■	■			■			■	■	■						
LG-10- 1	27.36860	89.34765	3801	Paro	gt-st schist																
LG-10- 2	27.38022	89.35152	3485	Paro	gt-bi schist																
LG-10- 3	27.31803	89.53805	2198	Paro	gt-ky-rutile schist	■				■	■	■	■	■		■	■		■		
LG-10- 4	27.31811	89.53759	2132	Paro	gt-ky schist		■	■			■	■	■							■	
LG-10- 5	27.53674	89.99506	1734	GHS	orthogneiss																
LG-10- 7	27.54029	90.00484	1734	TSS	bi-mu leucosome																
LG-10- 13	27.59578	90.31317	3090	TSS	gt-st schist	■			■	■	■	■	■	■		■					
LG-10- 33	27.71674	90.28676	4383	Leucogranite	bi-tur leucogranite					■	■	■	■		■						
LG-10- 46	27.79387	90.28486	4506	Leucogranite	mu-bi leucogranite					■	■		■								
LG-10- 48	27.80159	90.29220	4414	Leucogranite	gt-tur leucogranite	■				■	■		■		■						
LG-10- 49a	27.76340	90.32147	3999	Leucogranite	bi-mu leucogranite					■	■	■	■		■						
LG-10- 49b	27.76340	90.32147	3999	Leucogranite	bi-pegmatite					■	■		■		■		■		■		
LG-10- 49c	27.76340	90.32147	3999	Leucogranite	tur-gt pegmatite						■	■	■		■						
LG-10- 49d	27.76340	90.32147	3999	TSS	schist					■	■		■		■						
LG-10- 49e	27.76340	90.32147	3999	Leucogranite	gt pegmatite					■	■		■		■	■					
LG-10- 52a	27.74268	90.33025	3956	Leucogranite	tur pegmatite	■				■	■		■		■						
LG-10- 52b	27.74268	90.33025	3956	Leucogranite	pegmatite	■					■		■		■						
LG-10- 52c	27.74268	90.33025	3956	TSS	schist	■				■	■		■		■						
LG-10- 54	27.74023	90.32638	4300	TSS	gt-st schist	■				■	■	■	■	■		■					
LG-10- 55a	27.73667	90.32356	4308	TSS	quartzite																
LG-10- 55b	27.73667	90.32356	4308	TSS	quartzite																
LG-10- 58	27.73001	90.32151	4325	TSS	bi-qtz phyllite																
LG-10- 60a	27.73944	90.31499	4746	TSS	gt-st schist					■	■	■	■								
LG-10- 60b	27.73944	90.31499	4746	TSS	gt-st schist	■				■	■		■	■		■					
LG-10- 61	27.73629	90.31307	4635	TSS	gt-mu marble					■	■		■	■						■	
LG-10- 62	27.72600	90.30129	4593	TSS	bi phyllite					■		■	■								
LG-10- 65	27.46604	89.71371	2733	GHS	sill schist	■	■			■	■		■		■						
LG-10- 66a	27.44394	89.64553	2660	GHS	ox amphibolite		■	■										■			■
LG-10- 66b	27.44394	89.64553	2660	GHS	fuchsite sill schist		■			■	■		■		■					■	
LG-10- 70	27.09075	89.53486	2234	GHS	mylonitic bi-qtz schist	■				■	■		■	■	■						
LG-10- 73	27.07627	89.54495	2036	GHS	mylonitic bi-qtz schist	■	■	■		■	■	■	■								
LG-10- 77	27.07511	89.55288	1969	GHS	mylonitic bi-qtz schist																
LG-10- 81	27.06989	89.55556	1916	GHS	mylonitic bi-qtz schist	■	■	■		■	■		■	■	■						
LG-10- 83	27.06619	89.55353	1582	GHS	mylonitic bi-qtz schist	■		■		■	■		■		■						
LG-10- 85	27.05175	89.56054	1639	TSS	laminated quatzite					■	■		■		■		■		■		
LG-10- 86	27.04885	89.56806	1682	TSS	green quartzite	■				■	■	■	■		■						
LG-10- 87a	27.04453	89.57191	1712	TSS	quartzite					■	■		■		■				■		
LG-10- 87b	27.04453	89.57191	1712	TSS	pegmatite					■			■	■	■	■					
LG-10- 89	27.03349	89.58293	1779	TSS	mylonitic bi-qtz schist	■				■			■		■	■					
LG-10- 90	27.03248	89.58401	1798	TSS	qtz-fsp-bi-gt schist	■				■	■		■		■	■					
LG-10- 91	27.02777	89.58907	1833	GHS	mylonitic bi-qtz schist	■				■	■	■	■	■	■						
LG-10- 96	27.02077	89.56394	1933	GHS	mylonitic bi-qtz schist																
LG-10- 100	27.04991	89.56950	1595	TSS	calc schist	■				■					■				■		■

2 Metapelitic sample descriptions

In this section metapelitic samples from various units in Bhutan are described in detail.

LG-09-1

Location

LG-09-1 is an *in-situ* sample of GHS collected within a few kilometres of the basal GHS contact with Paro metasediments from a road section east of Wangdue in central Bhutan.

Assemblage and textures

LG-09-1 has a mineral assemblage of garnet, plagioclase, potassium feldspar, muscovite, biotite, quartz, tourmaline, apatite and ilmenite. Garnet porphyroblasts are <1 mm in diameter and sub-rounded. Inclusions of randomly-distributed quartz within the garnet porphyroblasts are <0.1 mm in diameter.

Plagioclase forms a common matrix phase and contains inclusion of quartz. The matrix is dominated by irregular bands which are alternately quartz-absent and quartz dominant, <0.2 – 5 mm wide.

Zoning and composition

Garnet from this sample shows subtle chemical zonation. Most of the grain shows no variation in chemistry, however the outer ~25 µm shows slight variation. The almandine content is approximately constant at $X_{alm} \approx 0.67$ throughout the grain. The pyrope content is approximately constant at $X_{py} \approx 0.11$ decreasing at the rim to $X_{py} \approx 0.09$. The spessartine content is approximately

constant at $X_{spss} \approx 0.17$ increasing towards the rim to $X_{spss} \approx 0.20$. The grossular content is constant throughout the grain at $X_{gr} \approx 0.05$.

Biotite grains are unzoned with a constant chemistry of $X_{Fe} \approx 0.60$, muscovite varies between $X_{Fe} \approx 0.62 – 0.68$ and plagioclase analyses show a fairly constant chemistry of $X_{Ca} \approx 0.27$.

Deformation history

The compositional banding within this sample suggests that this rock has experienced pervasive deformation.

Retrogression

The absence of chlorite and mineral breakdown textures suggest that this sample has not experienced retrogression. Garnet is partially resorbed.

LG-09-6

Location

LG-09-6 is an *in-situ* sample of GHS within a few kilometres of the top GHS contact, collected from a road section west of Trongsa in central Bhutan.

Assemblage and textures

LG-09-6 has an assemblage of garnet, staurolite, sillimanite, kyanite, plagioclase, muscovite, biotite, quartz, tourmaline and ilmenite. Garnet porphyroblasts are <3 mm in diameter and sub-rounded. Inclusions of quartz, staurolite, kyanite and ilmenite within the garnet porphyroblasts are <0.1 mm in diameter, common and randomly distributed (Fig5.4).

Porphyroblastic staurolite grains are measuring up to 3 mm in length and vary from elongate to equant in shape. Biotite, quartz, kyanite, garnet, graphite and ilmenite are found as inclusions in staurolite. Kyanite inclusions in staurolite are up to 0.3 mm across accompanied by quartz. Staurolites are concentrated in the mica-rich bands, exhibit sector zoning and are wrapped by the external fabric.

Kyanite laths between 0.3 and 1.5 mm in length are associated with mica-rich layers and staurolite. They are also found within pressure shadows and commonly share a crystal face with the staurolite (Fig. 5.4). Rare plagioclase is observed in the matrix. Biotite is found as elongate laths within mica-rich layers orientated parallel to the pervasive foliation and random orientations within the pressure shadows of staurolites. Muscovite is fine-grained and foliation parallel while quartz-rich regions are constituted of smaller subgrains. Fibrolitic sillimanite is present as irregular patches associated with biotite, it is common on some foliation surfaces in hand specimen. The matrix is dominated by quartz absent and quartz dominant irregular bands <0.2 – 5 mm wide.

Zoning and composition

Garnet shows no chemical zonation except at the outer edge of the grain, <100 μm from the rim (Fig. 5.1 and Fig. 5.4f). The almandine content is fairly constant at $X_{alm} \approx 0.76$ with a very minor increase at the rim. The pyrope content is approximately constant at $X_{py} \approx 0.14$ decreasing to $X_{py} \approx 0.13$ at the rim. The spessartine content is approximately constant at $X_{spss} \approx 0.03$ increasing towards the rim to $X_{spss} \approx 0.06$. The grossular content is high in the core at $X_{gr} \approx 0.02$ increasing towards the rim to $X_{gr} \approx 0.05$. The single analysed garnet inclusion in staurolite has a chemistry of $X_{alm} \approx 0.75$, $X_{py} \approx 0.14$, $X_{spss} \approx 0.06$, $X_{gr} \approx 0.04$ similar to the composition of the rims of matrix garnet.

Biotite shows no systematic change in composition within each grain, however there is significant variation in chemistry between grains in different petrographic settings. Biotite grains within the matrix have $X_{Fe} \approx 0.51$, those included in kyanite have $X_{Fe} \approx 0.52$, grains included in staurolite show $X_{Fe} \approx 0.46 – 0.51$, and those included in garnet show $X_{Fe} \approx 0.41 – 0.42$.

Muscovite is unzoned but varies between location; matrix muscovite and muscovite inclusons in staurolite show $X_{Fe} \approx 0.41 – 0.47$ and muscovite inclusions in garnet show $X_{Fe} \approx 0.53$. Staurolite preserves subtle change in chemistry from the core showing $X_{Fe} \approx 0.80$ to the rims showing $X_{Fe} \approx 0.85$, staurolite inclusions in garnet show $X_{Fe} \approx 0.79$ - 0.80. Plagioclase within the matrix yields a fairly constant chemistry of $X_{Ca} \approx 0.19$ while grains included in garnet exhibit $X_{Ca} \approx 0.25$.

Deformation history

The variety of inclusions found within different phases in this rock indicates a complicated growth and deformational history. Kyanite and staurolite inclusions within garnet suggest that these two phases were present before or during the first phases of garnet growth. Kyanite and garnet inclusions within staurolite suggest that these two phases were present before or during staurolite growth. Barring these inclusions being a 3D effect of the way the thin section was cut, the simplest solution for these textures is that there were two phases of staurolite growth at kyanite grade: an early phase of growth, with the grains subsequently included in garnet, and a later phase of growth which itself included garnet. Alternatively there are two phases of garnet growth: an early phase which got overgrown by staurolite and a later phase which overgrew some of the staurolite. The staurolites and garnets are both wrapped by the external fabric so must have grown pre- or syn-deformation.

Retrogression

The absence of chlorite indicates that little retrogression has occurred and the assemblage represents reasonable peak conditions. Garnet is partially resorbed.

LG-09-9

Location

LG-09-9 is an *in-situ* sample of TSS from the base of the klippen collected/sampled from a quarry on the roadside south of Trongsa in central Bhutan.

Assemblage and textures

It has a mineral assemblage of garnet, muscovite, biotite, plagioclase, quartz, tourmaline, apatite and ilmenite. Garnet porphyroblasts are rod-shaped; in sections parallel to dip direction they are euhedral, <3 mm in diameter and anhedral in sections orientated perpendicular to foliation and dip, <5 mm in length and commonly embayed. Inclusions of quartz and ilmenite are common but biotite is rare. The inclusions form straight trails within the garnet at an oblique orientation to the external fabric. At the garnet rims, there is some evidence for inclusions forming trails that are parallel to the external fabric.

Fine-grained quartz, muscovite, biotite and rare plagioclase make up the matrix. Plagioclase grains in the matrix are elongate and parallel to foliation. They are rare, anhedral and embayed. Mica and ilmenite are concentrated into bands parallel to the foliation that wraps the garnet porphyroblasts.

Zoning and composition

Garnet shows modest chemical zoning. The almandine content is lower in the core at $X_{alm} \approx 0.65$ increasing gradually towards the rims to $X_{alm} \approx 0.77$. The profile is smooth with no obvious breaks in composition. The pyrope content behaves similarly at lower modal proportions; $X_{py} \approx 0.06$ in the core increasing to $X_{py} \approx 0.12$ at the rim. In contrast, the grossular content is high in the core at $X_{gr} \approx 0.17$ decreasing towards the rim to $X_{gr} \approx 0.08$. The spessartine content is also higher in the core at $X_{spss} \approx 0.08$ decreasing towards the rim to $X_{spss} \approx 0.02$.

Biotite shows no systematic change in composition, $X_{Fe} \approx 0.52 – 0.54$. Muscovite is unzoned but varies with location; matrix muscovite shows $X_{Fe} \approx 0.52$ and muscovite inclusions in garnet show $X_{Fe} \approx 0.58$. Plagioclase is zoned, decreasing from $X_{Ca} \approx 0.43$ in the core to $X_{Ca} \approx 0.38$ at the rim.

Deformation history

Garnets are wrapped by a fabric defined by mica. The inclusion trail in garnet suggest that a pervasive deformational event occurred syn- and post-garnet rim growth rotating the garnet or two deformational events occurred, one recorded in the core of the garnet and a later event in the matrix foliation.

Retrogression

Sparse chlorite is localised around the vertices of garnets, associated with biotite. It is also found in small quantities within cracks in garnet. Although small volumes of chlorite are present, it is assumed that little retrogression has occurred and the assemblage represents reasonable peak conditions.

LG-09-32

Location

The highest sample in tectono-stratigraphic sequence, LG-09-32 was collected *in-situ* from a road cut between Zhemgang and Surey, on the order of 5 km structurally above the basal klippen contact.

Assemblage and textures

LG-09-32 contains garnet, muscovite, biotite, quartz, tourmaline and ilmenite. Euhedral garnet porphyroblasts are <3 mm in diameter. A second population of smaller, <0.3 mm diameter, rounded garnets are common in specific horizons. Inclusions of quartz, tourmaline and oxides form sigmoidal trails, which are mostly truncated relative to the external fabric. Biotite grains are commonly large and elongate, measuring up to 6 mm x 2 mm, and are generally orientated parallel to the pervasive foliation. Muscovite, quartz and ilmenite are included within subhedral, partly embayed biotite grains. Zircon, evident by the blackened haloes it causes, is common in biotite. The matrix is dominated by concentrated bands of muscovite and quartz <1 – 2 cm wide. Muscovite is fine-grained <0.2 mm with grains aligned to the foliation while parallel elongate quartz-rich regions are constituted of smaller subgrains. Plagioclase and potassium feldspar were very fine-grained and identified only under the electron microprobe. The feldspar grains analysed was found in the matrix adjacent to garnet.

Zoning and composition

Garnet shows clear and distinct chemical zoning. The almandine content is fairly constant at $X_{alm} \approx 0.4$ in the core, increasing gradually towards the rims where X_{alm} approaches 0.8. There is a slight jump in the almandine content at approximately 700 µm from the rim observable in the garnet

profile data. The pyrope content behaves similarly at lower modal proportions; $X_{py} \approx 0.02$ in the core and $X_{py} \approx 0.08$ at the rim. The spessartine content is high in the core at $X_{spss} \approx 0.35$ decreasing towards the rim to $X_{spss} \approx 0.08$. There is a distinctive jump in the spessartine content at ~700 µm from the rim from $X_{spss} \approx 0.33$ to $X_{spss} \approx 0.35$ before decreasing again towards the rim. This jump is also qualitatively observed in the element map. The grossular content is high in the core at $X_{gr} \approx 0.20$ decreasing towards the rim to $X_{gr} \approx 0.06$. In contrast to the spessartine and almandine profiles there is a dip in grossular content at ~700 µm from the rim decreasing from $X_{gr} \approx 0.20$ to $X_{gr} \approx 0.15$ before increasing then decreasing again from core to rim.

Biotite and muscovite show no systematic change in composition across the grains; biotite shows $X_{Fe} \approx 0.56$ and muscovite shows $X_{Fe} \approx 0.45 – 0.54$. The ilmenite composition is reasonably constant in the matrix; $X_{Ti} \approx 0.53$, however grains included in garnet are distinctly different exhibiting X_{Ti} up to 0.56. Plagioclase shows a constant composition of $X_{Ca} \approx 0.39$.

Deformation history

The muscovite in the matrix forms a clear crenulation cleavage with a spacing of ~3 mm indicating an early S1 foliation forming fabric and a late S2 crenulation. The crenulation is commonly focussed on the edges of the garnets and large biotites indicating S2 occurred after the growth of these two phases. Inclusion trails in biotite reflect the exterior foliation and suggest biotite growth post-S2.

A sharp change in the orientation of the inclusions within the garnet coinciding with an abrupt change in the chemistry indicated by the profile and element map indicate diversion from simple continuous prograde garnet growth. The inclusions trails appear to be continuous rather than truncated suggesting that the garnet did continue growing throughout the period. The change in

chemistry could be due to a change in available bulk rock chemistry such as the breakdown or growth of a new phase. The garnet became depleted in calcium and enriched in manganese and iron at this time; the growth of Ca-bearing phases such as apatite or allanite could be responsible.

Retrogression

Euhedral garnet and an absence of chlorite suggest that little retrogression has occurred and the assemblage represents reasonable peak conditions.

LG-09-41

Location

LG-09-41 is an *in-situ* sample from a road cut within the Chekha formation approximately 150 m structurally above the basal klippen contact near Surey.

Assemblage and textures, deformation history, retrogression

LG-09-41 contains garnet, muscovite, biotite. Garnet is sparse with grains are 3 x 2 mm and wrapped by the external fabric. Inclusions within the garnet are limited to graphite and a limited amount of ilmenite needles. The graphite is in very fine trails and outlines a fabric approximately parallel to the long axis of the garnet. It forms the outline of close packed parallel swathes of mica wrapping ~0.5 mm elongated areas devoid of graphite . The pattern gives the appearance of white mica wrapping plagioclase or quartz, however when observed in cross-polarised light it is obviously garnet. Ilmenite needles, ~0.1 mm in length, are sparse within the garnet but where they are seen are orientated perpendicular to the other internal fabric and are concentrated in the areas devoid of graphite .

Muscovite is concentrated in bands orientated in one of two directions distinct from the main foliation forming a herringbone pattern or an aligned series of grains of a single limb. It is inferred that the pattern is a result of crenulation cleavage which has been recrystallized elsewhere but still preserved in isolated areas. Biotite is sparse and present in the matrix parallel to the foliation.

Zoning and composition

Garnet in this sample shows distinct chemical zoning in a symmetric profile with no apparent jumps in chemistry. The almandine composition is lowest in the core at $X_{alm} \approx 0.52$ increasing towards the rim to $X_{alm} \approx 0.7$. The pyrope composition is generally low with a minimum in the core of $X_{py} \approx 0.05$ increasing up to $X_{py} \approx 0.12$ at the rim. The spessartine content varies the most significantly across the grain decreasing from $X_{spss} \approx 0.30$ in the core to $X_{spss} \approx 0.09$ at the rim. The grossular composition is reasonably constant at $X_{gr} \approx 0.13$ decreasing slightly in the outer ~500 μm to $X_{gr} \approx 0.10$.

Biotite shows approximate constant chemistry of $X_{Fe} \approx 0.53$, muscovite is unzoned ($X_{Fe} \approx 0.40$) and plagioclase shows approximate constant chemistry of $X_{Ca} \approx 0.29$.

Deformation history

The external fabric wraps the porphyroblast asymmetrically.

Retrogression

Garnet rim are coated in material of an orange-brown colour rich in iron indicating some degree of retrogression.

LG-09-43

Location

The most basal sample of TSS to the klippen contact near Surey, LG-09-43 is an *in-situ* sample of TSS from a road cut adjacent to GHS orthogneiss.

Assemblage and textures

LG-09-43 has a mineral assemblage of garnet, muscovite, biotite, tourmaline, quartz and ilmenite. Garnet is sparse and exists as elongate, inclusion-rich grains <2 x 3 mm, which are parallel to the fabric. The inclusions are mainly quartz.

Staurolite porphyroblasts <2 x 2 mm are common, especially in specific horizons and are associated with magnetite and muscovite. Staurolites contain inclusions of apatite, ilmenite and quartz, the inclusions form trails parallel to, and continuous with, the external fabric. Muscovite, biotite and ribbons of quartz define the foliation. There are large regions of quartz-dominated lenses <2 cm wide.

Zoning and composition

Garnet shows very limited chemical zoning. The profile is an asymmetric profile with no apparent jumps in chemistry. The almandine composition is marginally lower in the core at $X_{alm} \approx 0.77$ increasing towards the rim to $X_{alm} \approx 0.77$. The pyrope composition is approximately constant at $X_{py} \approx 0.1$. The spessartine content is generally low decreasing from $X_{spss} \approx 0.06$ in the core to $X_{spss} \approx 0.03$ at the rim. The grossular composition is reasonably constant at $X_{gr} \approx 0.06$.

Ilmenite composition varies according to microstructural position; within the matrix $X_{Ti} \approx 0.48$ whereas in staurolite $X_{Ti} \approx 0.44$. Muscovite and biotite show no variation in chemistry; in muscovite $X_{Fe} \approx 0.71$ and biotite $X_{Fe} \approx 0.53$. Staurolite shows no variation in chemistry; $X_{Fe} \approx 0.83$.

Deformation history

Inclusions trails of ilmenite in staurolite indicate that there were either two deformation events, or one which rotated the staurolite grains.

Retrogression

Well-formed chlorite is common in this sample. It is concentrated along one deformation plane that is inferred to have allowed fluid flow at a late stage in the rocks history. Garnet is partially resorbed.

LG-09-50

Location

LG-09-50 is an *in-situ* sample of GHS collected from a road section near Surey in south central Bhutan, approximately 2.5 km from both the basal and overriding contacts in the narrow expanse of GHS at Surey.

Assemblage

It has a mineral assemblage of garnet, plagioclase, biotite, muscovite, quartz, tourmaline and ilmenite. Garnets are small measuring <700 μm in diameter, inclusions of quartz, plagioclase, ilmenite and biotite are randomly orientated. Grains are rounded and confined to a densely

populated layer. Muscovite and biotite are commonly intergrown and form the foliation. Quartz and plagioclase form ribbons and grains parallel to foliation.

Zoning and composition

Garnet shows no chemical zoning except at the outer 20 µm rim in some grains. The almandine composition is approximately constant at $X_{alm} \approx 0.75$. The pyrope composition is approximately constant at $X_{py} \approx 0.13$ with a slight decrease at the rim. The spessartine content is approximately constant at $X_{spss} \approx 0.04$ with a slight increase at the rim. The grossular content is approximately constant at $X_{gr} \approx 0.06$.

Plagioclase shows no chemical zonation, however grains in the matrix have a higher proportion of sodium $X_{Na} \approx 0.80$ compared to inclusions in garnet ($X_{Na} \approx 0.73$). Muscovite and biotite are unzoned; muscovite shows $X_{Fe} \approx 0.42$ and biotite has $X_{Fe} \approx 0.52$.

Deformation history

The main foliation in the rock suggests that at least one phase of pervasive deformation has occurred. Micaceous bands partly wrapping the garnet and the randomly orientated inclusions suggest that garnet growth was pre-tectonic.

Retrogression

The lack of chlorite suggests little retrogression has occurred. Garnet is partially resorbed.

LG-09-60

Location

LG-09-60 is an *in-situ* sample of Jaishidanda from a road section ~8.5 km north west of Sarpang.

Assemblage

LG-09-60 is a moderately foliated schist which contains garnet, plagioclase, biotite, muscovite, ilmenite, tourmaline, apatite and quartz. Garnet porphyroblasts are <2 mm in diameter, subhedral and embayed, they are wrapped by the external fabric producing pressure shadows. Inclusions within garnet are of quartz, muscovite, biotite and ilmenite, they form sigmoidal inclusion trails which truncate the external fabric. Biotite and muscovite are fine-grained and are orientated approximately parallel to foliation wrapping garnets and occupying the homogeneous matrix alongside fine-grained quartz; in some cases muscovite mantles garnet. Chlorite is limited to selected biotite breakdown. Plagioclase is subhedral but stable in the assemblage.

Zoning and composition

Garnet from LG-09-60 shows clear and distinct chemical zonation exhibiting a low amplitude bell profile (Fig. 5.1). The almandine content is at a minimum in the core at $X_{alm} \approx 0.61$ increasing within ~600 µm to a constant value at $X_{alm} \approx 0.71$. The pyrope content is very low at $X_{py} \approx 0.03$ increasing towards the rim to $X_{py} \approx 0.06$. The spessartine content is at a maximum in core at $X_{spss} \approx 0.15$ decreasing constantly towards $X_{spss} \approx 0.02$ at the rim. The grossular content is approximately constant at $X_{gr} \approx 0.20$ throughout the grain.

Biotite is unzoned but composition varies between grains, one shows $X_{Fe} \approx 0.65$ and three grains show at $X_{Fe} \approx 0.55$. Muscovite is unzoned; $X_{Fe} \approx 0.43 – 0.51$ and plagioclase is zoned in one grain increasing from $X_{Ca} \approx 0.14$ in the core to $X_{Ca} \approx 0.20$ at the rim.

Deformation history

Garnet must have grown before the latest deformation event due to truncated inclusion trails. Plagioclase is stable and is not breaking down. Garnet is partially resorbed.

LG-09-61

Location

LG-09-61 is an *in-situ* sample from the base of the GHS, collected from a road section ~8.5 km north-west of Sarpang.

Assemblage and textures

LG-09-61 contains garnet, staurolite, plagioclase, muscovite, biotite, quartz, tourmaline, ilmenite, rutile and apatite. Garnet porphyroblasts are up to 2 mm x 4 mm across and subhedral to rounded. Inclusions of quartz, staurolite, ilmenite, biotite, rutile and muscovite are common. Quartz defines sigmoidal inclusion trails in the garnet cores. The inclusion trails are truncated by inclusion-poor rims <0.5 mm wide.

Biotite and muscovite define the foliation, which wraps the garnet; these minerals also occupy the pressure shadows. Matrix plagioclase forms anhedral, cracked grains <0.5 x 2 mm in size. Fluoro-apatite forms anhedral, cracked grains, <400 μm across, within the matrix and as inclusions in garnet. Quartz forms ribbons within the matrix; grains are deformed into subgrains of various sizes. Ilmenite within the matrix is <200 μm across, anhedral and sometimes contains a core of rutile.

Zoning and composition

Garnet is generally unzoned. The almandine content is approximately constant at $X_{alm} \approx 0.77$. There is a subtle decrease towards the rim increasing again at the very edge. The pyrope content is approximately constant at $X_{py} \approx 0.16$ decreasing at the rim to $X_{py} \approx 0.14$. The spessartine content is very low and approximately constant at $X_{spss} \approx 0.02$. The grossular content is approximately constant at $X_{gr} \approx 0.05$. The x-ray maps show that there is a chemically distinct rim growth on some edges of the grain overgrowing the original euhedral garnet; the chemistry of this rim, <500 μm wide, is $X_{alm} \approx 0.78$, $X_{gr} \approx 0.03 – 0.04$ with pyrope and spessartine contents as for the core of the garnet.

Biotites are not chemically zoned but their chemistry varies according to location; those in the matrix show $X_{Fe} \approx 0.53$, those within garnet show $X_{Fe} \approx 0.38 – 0.46$. Muscovite shows no consistent chemical zoning but chemistry does vary between grains; matrix muscovite shows $X_{Fe} \approx 0.42$ and two muscovite inclusions in garnet show $X_{Fe} \approx 0.45$ and 0.78. Plagioclase shows no consistent chemical variation across grains and shows $X_{Ca} \approx 0.13$. The composition of staurolite included in garnet varies from grain to grain from $X_{Fe} \approx 0.63 – 0.83$, there is no link between chemistry and distance to the rim of the garnet.

Deformation history

Garnet has had up to three phases of growth indicated by cores rich in inclusions which define a sigmoidal pattern, a subsequent growth period with randomly orientated inclusions and a final late stage of growth of low calcium content on faces perpendicular to foliation. Staurolite inclusions in garnet suggest that it grew before or during garnet growth.

Retrogression

Chlorite is absent from the assemblage and most phases appear stable suggesting no significant retrogressive effects have occurred. Garnet is partially resorbed.

LG-09-70

Location

LG-09-70 is a pebble sample of GHS collected from the confluence of a north-draining and an east-draining river near Damphu in south central Bhutan. Although the origin of the sample is unknown, it matches the description of kyanite-bearing schists described by Gansser from the Black Mountains to the east. The rarity of this lithology in the river at this location suggests either that the majority of this lithology has been weathered down or it is rare in the watershed area of this river. It is assumed that the sample is sourced from the eastern river and therefore part of the southern narrow expanse of GHS extending across to Surey south of the Black mountains.

Assemblage

LG-09-70 is well-foliated with an assemblage of garnet, kyanite, plagioclase, staurolite, muscovite, biotite, quartz, apatite and ilmenite. Garnet porphyroblasts are <3 mm in diameter, subhedral and fractured with randomly-oriented inclusions of quartz, staurolite, chlorite, apatite and biotite. Kyanite forms euhedral and lath-like crystals, with inclusions of biotite and muscovite. Staurolite is porphyroblastic, <2 mm across and contains only rare inclusions of quartz. Muscovite and biotite form laths parallel to the foliation, as well as forming in more random orientations. Quartz- and plagioclase-rich lenses are wrapped by bands rich in aluminous phases.

Zoning and composition

Garnet shows subtle chemical zonation. The core shows constant chemistry while the outer ~50 µm shows slight variation. The almandine content is approximately constant at $X_{alm} \approx 0.78$ increasing to $X_{alm} \approx 0.80$ at the rim. The pyrope content is approximately constant at $X_{py} \approx 0.15$ decreasing at the rim to $X_{py} \approx 0.12$. The spessartine content is approximately constant at $X_{spss} \approx 0.05$ throughout the grain. The grossular content is constant throughout the grain at $X_{gr} \approx 0.02$.

Biotite is unzoned but varies in chemistry between location; biotite in the matrix shows $X_{Fe} \approx 0.51$ - 0.54, biotite in garnet shows $X_{Fe} \approx 0.48$ and biotite in kyanite shows $X_{Fe} \approx 0.47$ - 0.49. Muscovite is unzoned but varies in chemistry between $X_{Fe} \approx 0.50 – 0.58$, independent of location. Plagioclase and staurolite are unzoned; plagioclase shows $X_{Ca} \approx 0.09$, staurolite shows $X_{Fe} \approx 0.83$.

Deformation history

The randomly orientated phases indicate that although there is some compositional banding with limited aligned phases, this rock did not experience pervasive deformation during all of its prograde mineral growth.

Retrogression

The presence of chlorite associated with biotite and a thin orange iron-rich film along fractures in and around garnet indicates a limited degree of retrogression. Garnet is partially resorbed.

LG-09-85

Location

LG-09-85 is an *in-situ* sample of GHS from the contact between GHS and Paro metasediments in the Wangdue window, collected from a road section ~3 km south of Wangdue.

Assemblage

LG-09-85 is fine- to medium-grained with weak foliation, containing garnet, plagioclase, muscovite, biotite, sillimanite, chlorite, apatite, ilmenite and quartz. There is a lack of compositional banding. Garnets <2 mm in diameter are rounded and contains abundant randomly orientated inclusions of biotite, muscovite, and quartz <0.5 mm in size.

Within the matrix plagioclase is sparse, anhedral, fractures and <0.2 mm across. Biotites are both randomly orientated and form a faint foliation, they form <1 mm laths. Sillimanite is sparse and present as bundles of fibrolite. Garnet is partially resorbed.

Zoning and composition

The chemical zoning in garnet is obscured by the high volume of inclusions in the core. In most grains only the outer ~50 µm shows slight chemical variation. The almandine content is approximately constant at $X_{alm} \approx 0.80$ throughout the grain. The pyrope content is approximately constant at $X_{py} \approx 0.10$ decreasing slightly at the rim to $X_{py} \approx 0.09$. The spessartine content is approximately constant at $X_{spss} \approx 0.05$ increasing to $X_{spss} \approx 0.07$ at the rim. The grossular content is constant at $X_{gr} \approx 0.05$ throughout the grain. The profiles appear to vary slightly towards the inclusion-rich core.

Biotite is unzoned showing a slight compositional difference between grains in the matrix and included in garnet; biotite in the matrix shows $X_{Fe} \approx 0.67$ and biotite in garnet shows $X_{Fe} \approx 0.65$. Muscovite is unzoned and shows constant chemistry in different locations; $X_{Fe} \approx 0.64$. Plagioclase is zoned showing $X_{Ca} \approx 0.23$ in the core increasing to $X_{Ca} \approx 0.30$ at the rim.

Deformational history

A weak foliation is preserved and no compositional banding is seen in this sample indicating that it has experienced limited deformation.

Retrogression

A small proportion of biotite is altered to chlorite indicating limited retrogression. Garnet is partially resorbed.

LG-09-90

Location

LG-09-90 is an *in-situ* sample of GHS within a few hundred metres of the basal GHS contact with Paro metasediments in the Paro window, collected along a trekking route ~2 km south of Semtoka and 4.5 km structurally and physically below LG-09-98.

Assemblage

LG-09-90 is a well-foliated schist containing garnet, sillimanite, plagioclase, biotite, muscovite, ilmenite, quartz, tourmaline, chlorite and rutile. Garnet <2 mm across is rounded, fractured and contains inclusions of quartz, biotite, muscovite, chlorite, tourmaline and rutile. Fibrolitic sillimanite forms bundles parallel to foliation and associated with biotite. Biotite and muscovite form narrow laths parallel to foliation wrapping garnet grains. Feldspar shows exsolution and twinned textures in some cases.

Zoning and composition

Garnet shows subtle chemical zonation in the outer ~300 μm. The almandine content is approximately constant at $X_{alm} \approx 0.75$ decreasing very slightly to $X_{alm} \approx 0.74$ at the rim. The pyrope

content is approximately constant at $X_{py} \approx 0.16$ decreasing at the rim to $X_{py} \approx 0.09$. The spessartine content is approximately constant at $X_{spss} \approx 0.04$ increasing to $X_{spss} \approx 0.13$ at the rim. The grossular content is constant at $X_{gr} \approx 0.06$ decreasing to $X_{gr} \approx 0.04$ at the rim.

Biotite shows constant chemistry; $X_{Fe} \approx 0.59$, muscovite shows inconsistent variation within grains; $X_{Fe} \approx 0.50 – 0.54$. Plagioclase is unzoned with $X_{Ca} \approx 0.50$.

Deformation history

Alignment of sillimanite and biotite indicates pervasive deformation during sillimanite growth. Garnets wrapped by micas indicate pre-tectonic garnet growth.

Retrogression

Garnet has inclusions of chlorite and is coated in a thin film of orange iron-rich material indicating some degree of retrogression.

LG-09-98

Location

LG-09-98 is an *in-situ* sample of GHS within a few kilometres of the basal GHS contact with Paro metasediments in the Paro window. It was collected along a trekking route ~1.5 km north-west and structurally and topographically lower than sample LG-09-101.

Assemblage

This sample contains garnet, plagioclase, potassium feldspar, biotite, muscovite, sillimanite, quartz and ilmenite. The rock is banded on a 3-5 mm scale with alternating quartz- and mica-dominated

regions. Garnet is <1.5 mm across, embayed and anhedral containing randomly orientated inclusions of quartz, biotite and potassium feldspar. Fibrolitic sillimanite forms bunches lying parallel to the foliation. Biotite grains are <1 mm across, muscovite is finer-grained and sparse. Plagioclase is fractured and anhedral in grains <0.5 mm across.

Zoning and composition

Only the outer ~100 μm of garnet is chemically zoned. The almandine content is approximately constant at $X_{alm} \approx 0.69$ decreasing very slightly to $X_{alm} \approx 0.70$ at the rim. The pyrope content is approximately constant at $X_{py} \approx 0.10$ decreasing at the rim to $X_{py} \approx 0.08$. The spessartine content is approximately constant at $X_{spss} \approx 0.17$ increasing to $X_{spss} \approx 0.20$ at the rim. The grossular content is constant throughout the grain at $X_{gr} \approx 0.03$.

Biotite is unzoned and has the same composition where it is included in garnet and in the matrix; $X_{Fe} \approx 0.63$. Muscovite is unzoned and varies between $X_{Fe} \approx 0.55$ - 0.68. Plagioclase is unzoned and varies between $X_{Ca} \approx 0.19$ - 0.23. Potassium feldspar is unzoned and shows $X_{Na} \approx 0.10$.

Deformation history

A strong foliation indicates at least one period of pervasive deformation.

Retrogression

A lack of chlorite indicated limited retrogression have occurred. Garnet is partially resorbed.

LG-09-101

Location

LG-09-101 is an *in-situ* sample of GHS collected along a trekking route ~7 km south of Semtoka, within a few kilometres of the basal GHS contact with Paro metasediments in the Paro window.

Assemblage

This sample has an assemblage of biotite, muscovite, potassium feldspar, sillimanite, quartz and apatite. It is relatively course-grained and is poorly foliated. Reddish biotite forms large euhedral grains <3 mm across. Fibrolitic sillimanite forms randomly orientated bundles parallel to the foliation and is sometimes associated with biotite. Potassium feldspar is found infilling around quartz grains.

Zoning and composition

Biotite and potassium feldspar are unzoned and shows $X_{Fe} \approx 0.6$. Muscovite is unzoned and shows $X_{Fe} \approx 0.48 – 0.51$.

Deformation history

Folded foliation indicates at least two phases of deformation.

Retrogression

Plagioclase is altered in patches indicating that some degree of retrogression may have occurred.

LG-10-3

Location

From a road section ~1 km west of the confluence, LG-10-3 is an *in-situ* sample from the Paro metasediments within the Paro Window.

Assemblage and textures

LG-10-3 has a mineral assemblage of garnet, kyanite, plagioclase, muscovite, biotite, quartz, tourmaline, rutile and ilmenite. Garnet porphyroblasts are <6 mm in diameter, subhedral and embayed. Inclusions of quartz, biotite and ilmenite within the garnet porphyroblasts are <0.1 mm in diameter and common. The inclusions form sigmoidal trails in the core of the garnet, while inclusion trails in the rim are approximately straight. Both fabrics within the garnet truncate the external fabric. Kyanite laths <5 mm in length were observed in outcrop and hand specimen, smaller grains are observed in thin section. Grains exhibit classic cleavages and have a blue tint to otherwise colourless laths. Rare, fine-grained plagioclase is found in the matrix. Biotite is found as elongate laths within mica-rich layers orientated parallel to the pervasive foliation and random orientations within the pressure shadows of garnets. Muscovite is found as elongate laths within the matrix defining the foliation and wrapping garnet. Quartz-rich regions are constituted of smaller subgrains.

Zoning and composition

Biotite shows no systematic change in composition across the dimensions of grains, however there is significant variation in chemistry between grains in different petrographic settings. Grains within the matrix generally contain equal proportions of Mg and Fe; $X_{Mg} \approx 0.49$ with some grains which contain proportions of Fe of up to 0.53. Biotites included in staurolite have a higher proportion of Mg compared to Fe; $X_{Mg} \approx 0.53$ while those included in garnet have an even higher proportion of Mg compared to Fe; $X_{Mg} \approx 0.58$. Those included in kyanite have a higher proportion of Fe than Mg; $X_{Mg} \approx 0.47$.

Garnet from LG-10-3 shows unique chemical zonation with a flat profiled core ~1000 µm in diameter and various zonation patterns in the outer ~700 µm of the grain (Fig. 5.1). The almandine content is at a minimum in the core at $X_{alm} \approx 0.81$ increasing to $X_{alm} \approx 0.90$ at the rim. The pyrope content is constant at $X_{py} \approx 0.12$ in the core increasing to a maximum ~250 µm from the rim to $X_{py} \approx 0.14$ then decreases to the rim to $X_{py} \approx 0.08$. The spessartine content is constant in the core at $X_{spss} \approx 0.01$ decreasing to $X_{spss} \approx 0.00$ in the outer ~500 µm of the grain. The grossular content is constant at $X_{gr} \approx 0.05$ in the core decreasing progressively in the outer ~500 µm of the grain to $X_{gr} \approx 0.00$ at the rim.

Deformation history

A lack of chlorite indicates that limited retrogression has occurred. Garnet is partially resorbed.

Retrogression

Euhedral garnet and an absence of chlorite indicate that little retrogression has occurred and the assemblage represents reasonable peak conditions.

LG-10-13

Location

LG-10-13 is an *in-situ* sample of TSS from a small exposure crossing the path in the Nikha Chu valley in north central Bhutan. This sample lies approximately 100m above the inferred basal klippen contact with orthogneiss from the GHS and cliffs densely veined by leucogranite structurally below.

Assemblage and textures

LG-10-13 has a peak assemblage of garnet, staurolite, plagioclase, muscovite, biotite, quartz, tourmaline and ilmenite. Garnet porphyroblasts are <1.5 mm in diameter, subhedral and embayed. Inclusions of quartz and ilmenite within the garnet porphyroblasts <0.1 mm in diameter are common. The inclusions form poorly defined sigmoidal trails in the core of the garnet and are approximately consistent with the external fabric. Staurolite is commonly found in association with garnet, it is poikiloblastic and embayed. Rare, fine-grained plagioclase is found in the matrix. Muscovite and biotite are orientated parallel to the pervasive foliation, wrapping garnets and in random orientations within the pressure shadows of garnets. Quartz-rich regions are constituted of smaller subgrains.

Zoning and composition

Garnet shows an asymmetric element profile with minor chemical zoning. The almandine content is lowest in the core at $X_{alm} \approx 0.65$ increasing towards the rims to $X_{alm} \approx 0.78$. The pyrope composition is reasonably constant; $X_{py} \approx 0.07$ in the core and $X_{py} \approx 0.1$ at the rim. The spessartine content shows significant variation across the grain with a maximum in the core at $X_{spss} \approx 0.21$ decreasing towards the rim to $X_{spss} \approx 0.07$. The grossular content is reasonably constant across the grain at $X_{gr} \approx 0.05$.

Biotite, muscovite and staurolite are unzoned; biotite shows $X_{Fe} \approx 0.55$, muscovite shows $X_{Fe} \approx 0.63$, staurolite shows $X_{Fe} \approx 0.85$. Plagioclase varies between $X_{Ca} \approx 0.17 – 0.23$.

Deformation history

A single deformation event can be deduced from the garnet wrapped by an external fabric approximately coincident with the internal garnet fabric.

Retrogression

Euhedral garnet and an absence of chlorite indicate that little retrogression has occurred and the assemblage represents reasonable peak conditions.

LG-10-54

Location

The most northerly sample of TSS collected in this study, LG-10-54 is an *in-situ* sample of garnet mica schist collected from a narrow exposure, <50m thick, structurally below a massive expanse of TSS carbonate and above the <1 km thick Gophu La leucogranite.

Assemblage and textures

LG-10-54 has an assemblage of garnet, plagioclase, muscovite, biotite, ilmenite, quartz and tourmaline. Garnet porphyroblasts are <1 cm across are wrapped by the external fabric. Inclusions within garnet are of quartz, chlorite, muscovite, biotite and graphite. They form sigmoidal trails that are truncated by the external fabric. Graphite in particular defines complex inclusion trails and suggests that the rock fabric was previously crenulated. Muscovite and biotite define the foliation. Some biotite grains cross-cut the fabric.

Zoning and composition

Garnet preserves clear and distinct chemical zoning. The almandine composition increases from the core to the rim (X_{alm} ≈ 0.55-0.70). The pyrope composition is very low (X_{py} ≈ 0.03) and approximately constant through the core, although increases to X_{py} ≈ 0.05 at the rim. The

spessartine content is at a maximum in the core at $X_{spss} \approx 0.28$ decreasing to $X_{spss} \approx 0.08$ at the rim. The grossular content is high in the core at $X_{gr} \approx 0.12$ increasing towards the rim to $X_{gr} \approx 0.18$.

Plagioclase shows no consistent zoning; however the chemistry varies between $X_{Ca} \approx 0.73 – 0.89$ independent of position. Biotite is unzoned and shows $X_{Fe} \approx 0.68$, muscovite is unzoned but shows variation between locations; matrix muscovite shows $X_{Fe} \approx 0.67$ and muscovite inclusions in garnet show $X_{Fe} \approx 0.80$

Deformation history

S1 is preserved within the garnets in graphite trails, garnet grew post S1 and an S2 fabric is preserved in the foliation wrapping the garnets.

Retrogression

Chlorite is confined to the rims and as inclusions within garnet. Although the inclusion could be primary growth of chlorite the chlorite on the rims of garnet is inferred indicated limited retrogression. Garnet is partially resorbed.

LG-10-65

Location

LG-10-65 is an *in-situ* sample of GHS collected from a road section east of Thimphu in west central Bhutan within a few hundred metres of the basal GHS contact with Paro metasediments in the Paro window.

Assemblage

LG-10-65 is a medium-grained folded paragneiss containing garnet, sillimanite, plagioclase, potassium feldspar, muscovite, biotite and quartz. Garnet is <1 mm in diameter and contains inclusions of quartz, plagioclase and muscovite in the core. Biotite and muscovite grains are <1mm across and form the dominant matrix phases with feldspar and quartz. Fibrolitic silimanite is associated with biotite.

Zoning and composition

Garnet from this sample shows subtle chemical zonation. The almandine content is at $X_{alm} \approx 0.72$ in the core decreasing gradually towards the rim to $X_{alm} \approx 0.68$. The pyrope content in the core is at $X_{py} \approx 0.12$ decreasing gradually to $X_{py} \approx 0.10$ at the rim. The spessartine content is at a minimum in the core at $X_{spss} \approx 0.11$ increasing towards the rim to $X_{spss} \approx 0.18$. The grossular content is variable at low concentrations. The core of the garnet is at a minimum at $X_{gr} \approx 0.04$ increasing to $X_{gr} \approx 0.06$ half way between the core and rim before decreasing to $X_{gr} \approx 0.04$ at the rim.

Bioitite and potassium feldspar are unzoned; biotite shows $X_{Fe} \approx 0.60 – 0.63$. Muscovite is unzoned but varies independently between $X_{Fe} \approx 0.50 – 0.64$. Plagioclase is unzoned but shows variation between grains in different locations; matrix plagioclase shows $X_{Ca} \approx 0.12 – 0.20$ and plagioclase inclusions in garnet show $X_{Fe} \approx 0.23 – 0.35$.

Deformation history

The pervasive fabric is folded, suggesting that two deformation events affected this rock.

Retrogression

The absence of chlorite indicates that it has experienced little to no retrogression. Garnet is partially resorbed.

LG-10-83

Location

LG-10-83 is an *in-situ* sample of GHS structurally below a synformal "keel" of metasediments from a road section near Chukha in south west Bhutan. The metasediments in this area are considered to be part of the TSS.

Assemblage

This sample has a mineral assemblage of garnet, kyanite, biotite, muscovite, quartz, ilmenite and rutile. Garnets are <2 mm across and subhedral to rounded. Inclusions within the garnet are randomly orientated, relatively absent in outer 200 µm and consist of quartz, biotite, apatite, rutile and muscovite. Kyanite is euhedral to subhedral, <1 mm across and commonly randomly orientated with inclusions of biotite. Biotite is common and forms grains <1 mm across. This rock is poorly foliated although there are quartz-rich bands <1 cm across.

Zoning and composition

Garnet in this sample shows only subtle chemical zonation in the outer rim (<70 µm from the rim). The almandine composition is approximately constant at $X_{alm} \approx 0.77$ increasing to $X_{alm} \approx 0.79$ at the rim. The pyrope composition is approximately constant at $X_{py} \approx 0.15$ with a slight decrease at the rim to $X_{py} \approx 0.11$. The spessartine content is approximately constant at $X_{spss} \approx 0.03$ with a slight increase at the rim to $X_{spss} \approx 0.05$. The grossular content is approximately constant at $X_{gr} \approx 0.05$.

Biotite is unzoned but shows distinct chemical variation between location; matrix biotite shows X_{Fe} ≈ 0.57 and three groups of biotite inclusions in garnet show X_{Fe} ≈ 0.47, 0.50 and 0.55.

Deformation history

Compositional banding, despite a lack in parallel aligned grains, shows that deformation is limited in this sample.

Retrogression

There is no chlorite present in this sample and little sign of mineral breakdown textures indicating that this rock has not experienced any significant retrogressive effects. Garnet is partially resorbed.

3. Garnet profiles

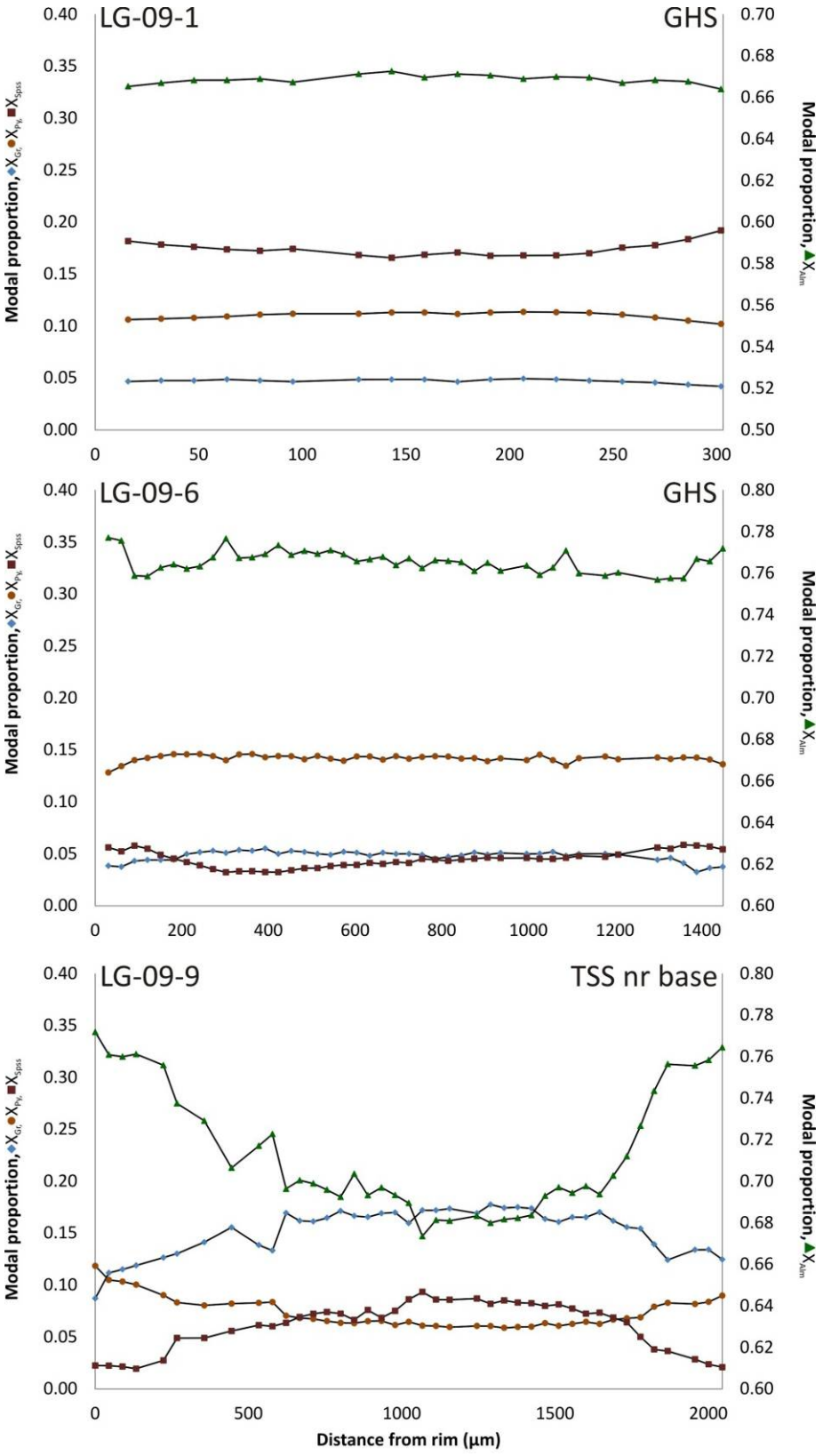

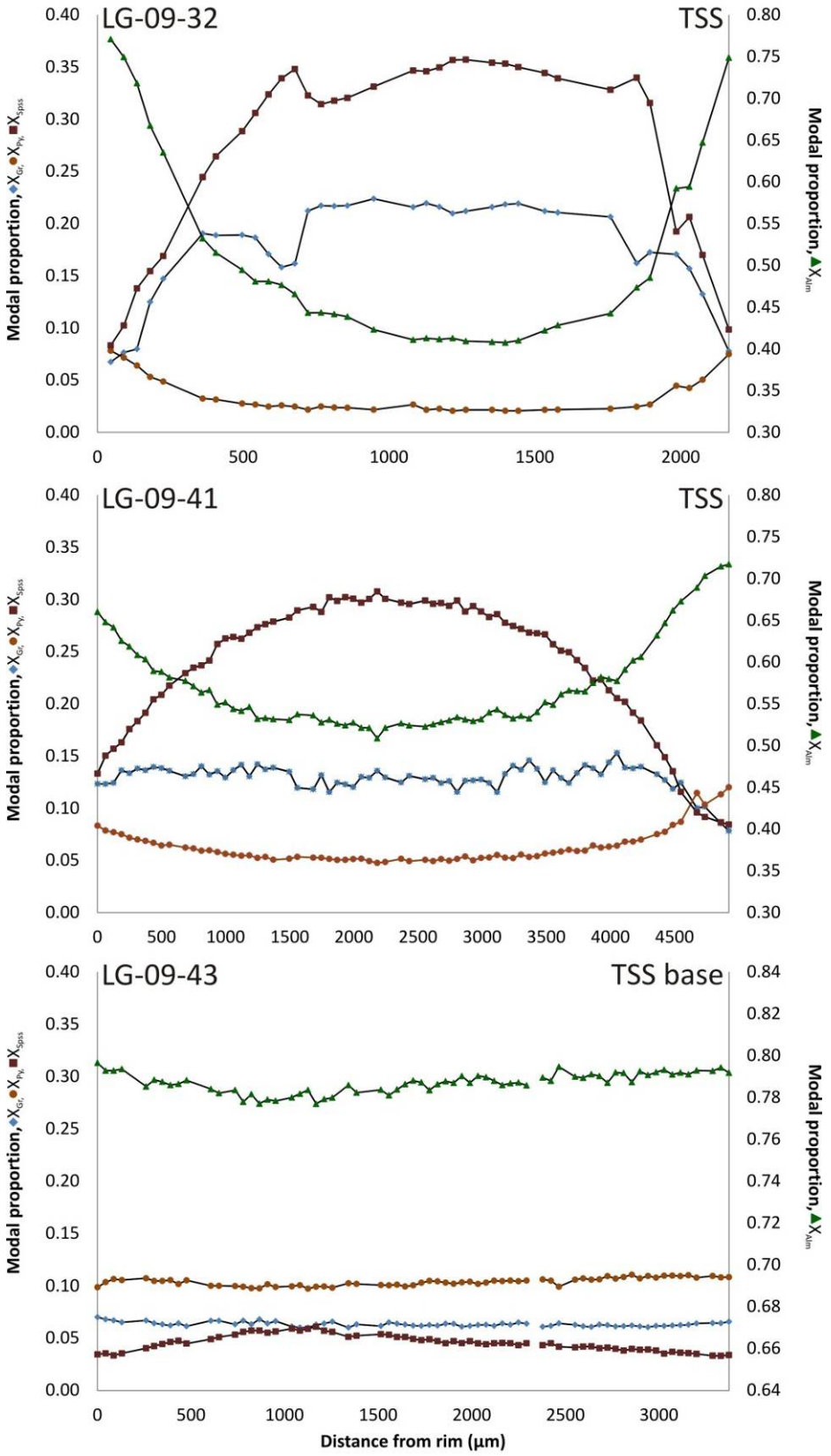
LG-09-32
TSS
LG-09-41
TSS
LG-09-43
TSS base
Modal proportion, ◆X_Gt, ●X_Py, ■X_Spss
Modal proportion, ▲X_Alm
Distance from rim (µm)

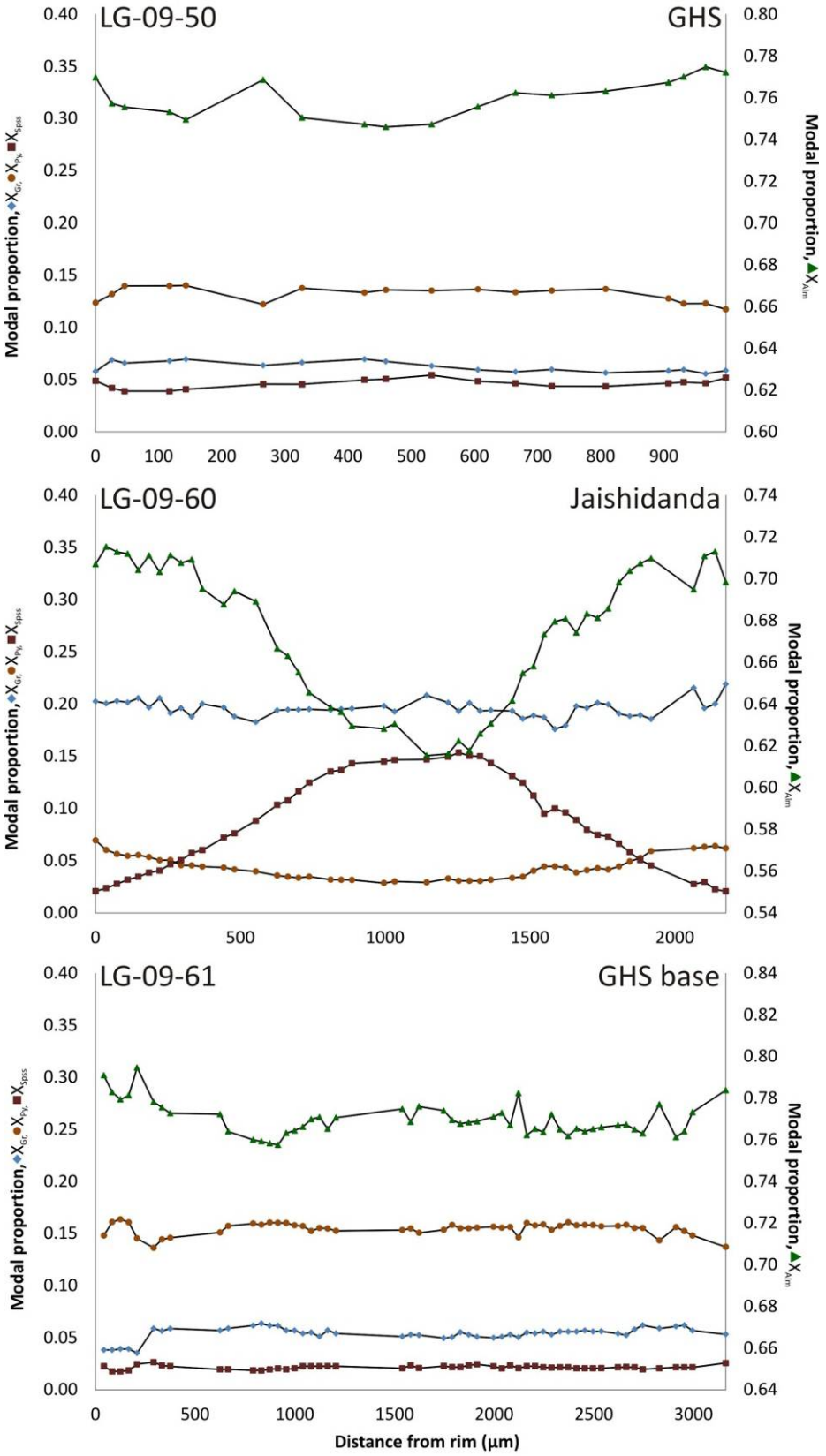
LG-09-50
GHS
Modal proportion, X_{Gr} X_{Py} X_{Spss}
Modal proportion, X_{Alm}
LG-09-60
Jaishidanda
LG-09-61
GHS base
Distance from rim (µm)

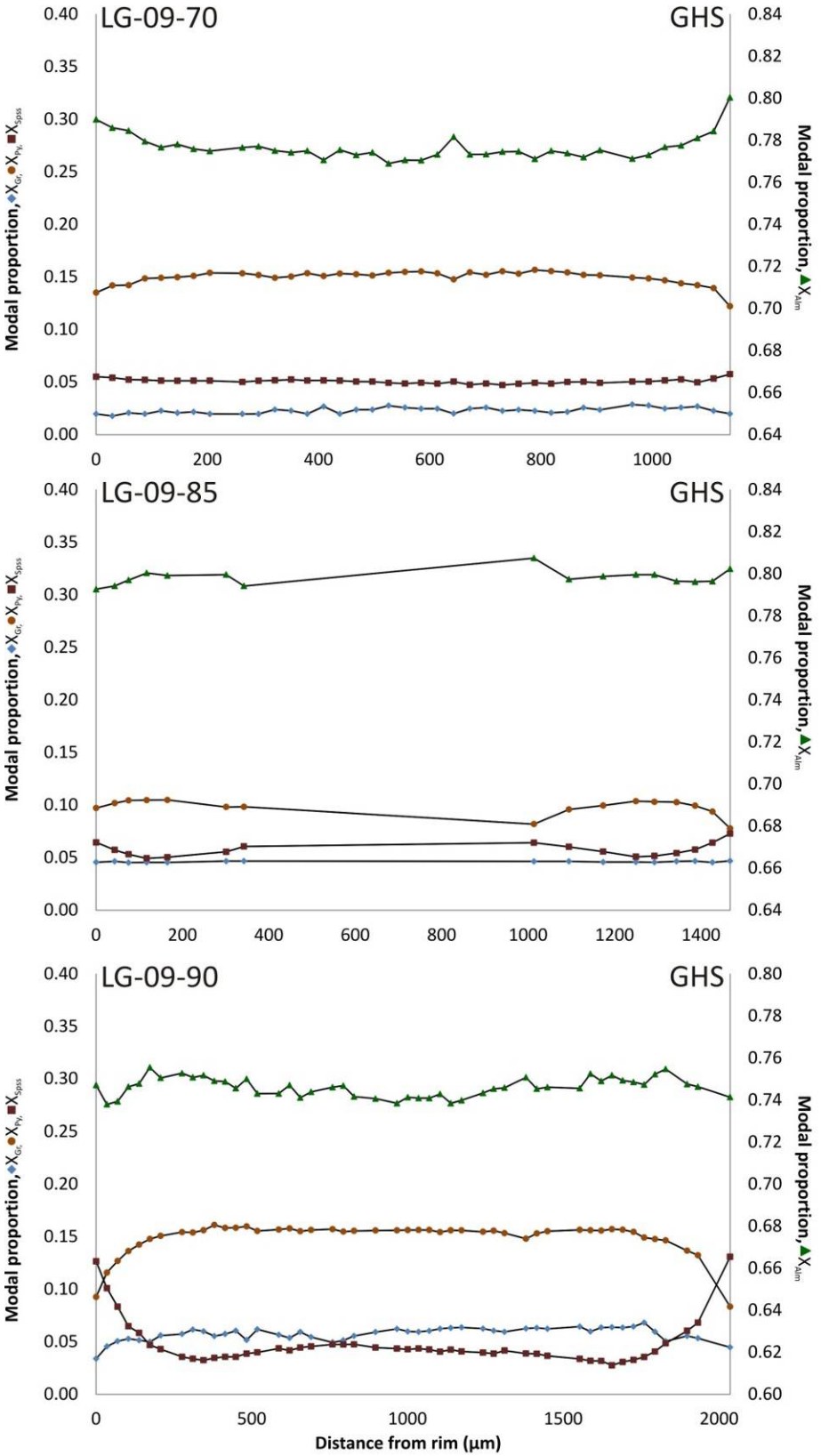
LG-09-70
GHS
LG-09-85
GHS
LG-09-90
GHS
Modal proportion, ◆X_{Gt}, ●X_{Hy}, ■X_{Spss}
Modal proportion, ▲X_{Alm}
Distance from rim (µm)

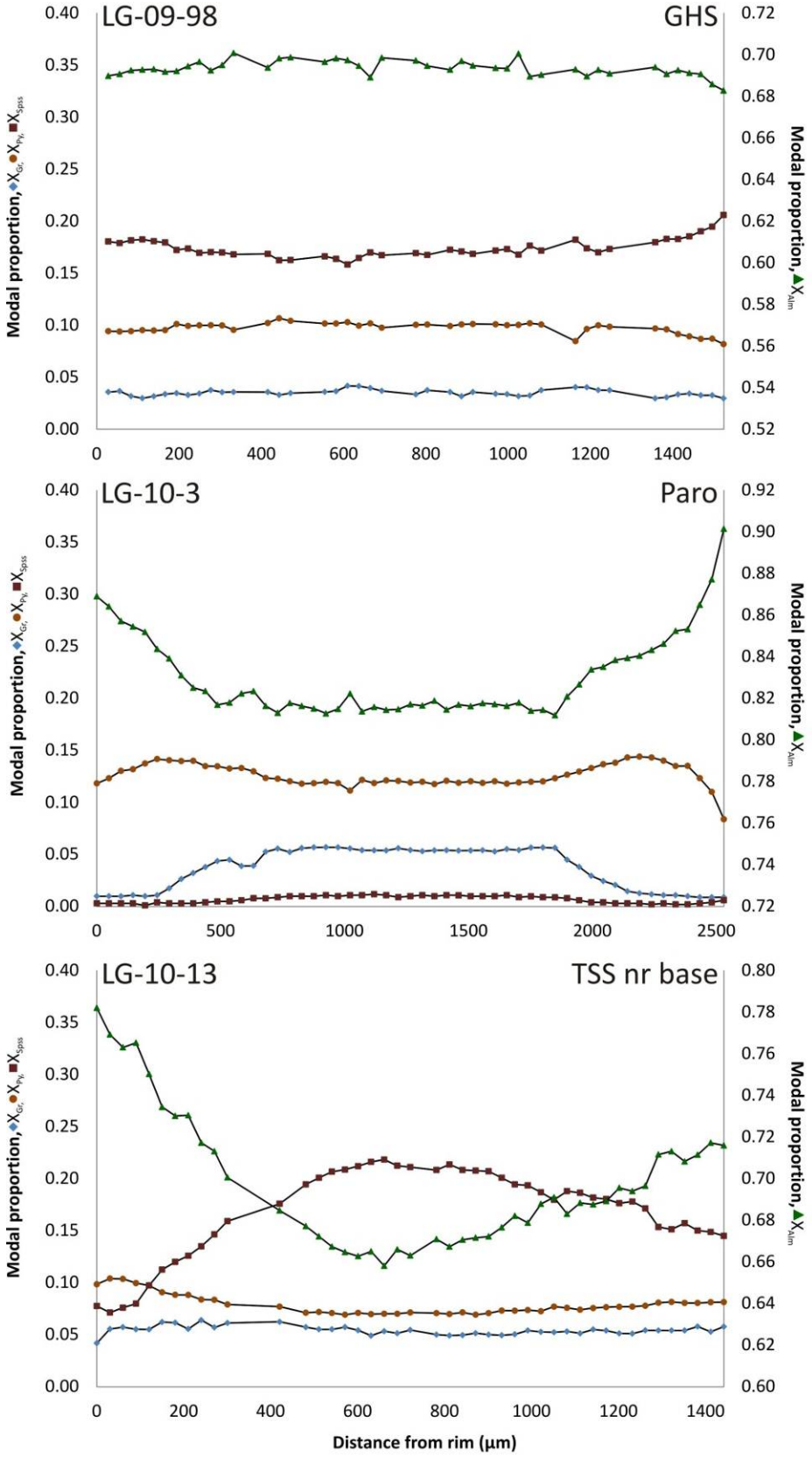
LG-09-98
GHS
LG-10-3
Paro
LG-10-13
TSS nr base
Modal proportion, ◆X_{Gt}, ●X_{Py}, ■X_{spss}
Modal proportion, ▲X_{Alm}
Distance from rim (µm)

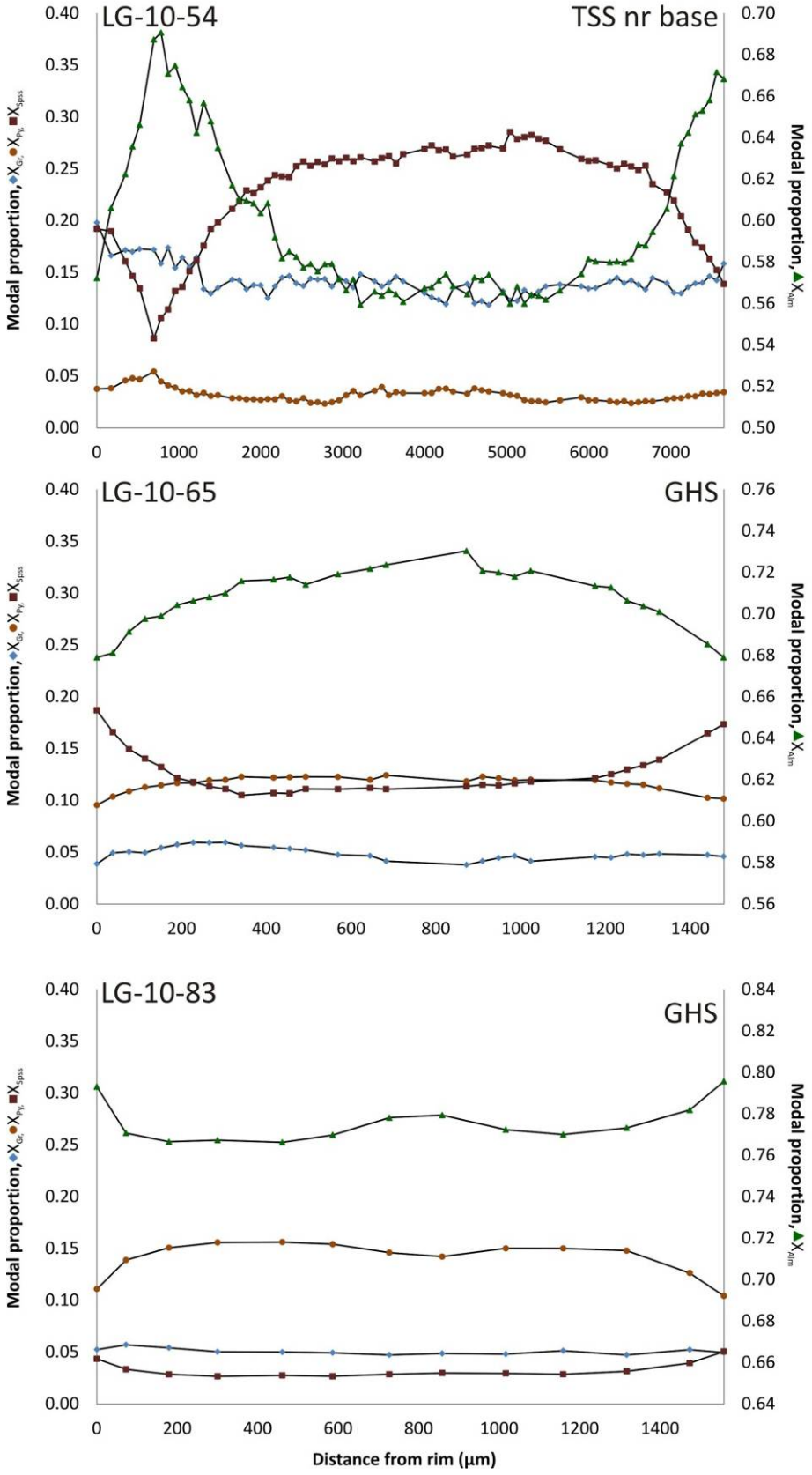
LG-10-54
TSS nr base
LG-10-65
GHS
LG-10-83
GHS
Modal proportion, ◆X_Gt, ●X_Py, ■X_Spss
Modal proportion, ▲X_Alm
Distance from rim (µm)

Figure B.1: Representative garnet chemical profiles from samples throughout Bhutan. Profiles are labelled with the unit they belong to and are in sample number order.